Segregation and the work function of a random alloy: PdAg(111)

1993 J. Phys.: Condens. Matter 5 L443

(http://iopscience.iop.org/0953-8984/5/36/003)

J. Phys.: Condens. Matter 5 (1993) L443–L448. Printed in the UK

LETTER TO THE EDITOR

Segregation and the work function of a random alloy: PdAg(111)

S Crampin†

Institute for Theoretical Physics, Catholic University of Nijmegen, Toernooiveld, NL-6525 ED Nijmegen, The Netherlands

Received 8 June 1993, in final form 29 July 1993

Abstract. Self-consistent parameter-free calculations of the surface electronic structure of a random alloy are used to discuss the compositional dependance of the work function (Φ) of the PdAg(111) random alloy surface. For crystals with uniform concentration profile Φ varies almost linearly between the pure metal limits, and in the presence of segregation is found to be a measure of the surface layer composition. Good agreement with measured polycrystalline work functions is found using experimentally determined segregation data. The results are used to understand screening within PdAg alloys and point to possible surface-alloy formation during the growth of Pd on Ag.

Random-alloy surfaces are of importance in surface chemistry where compositional variables are exploited to tailor properties or segregation used to concentrate expensive catalytic components. The complexity arising from compositional disorder prevents the application of theoretical techniques which can describe these surfaces with similar accuracy to that available for pure metal surfaces or simple adsorbate systems, but developments based upon the Korringa–Kohn–Rostoker coherent-potential approximation (KKRCPA) have enabled parameter-free, charge self-consistent calculations for bulk alloys comparable to multiple-scattering treatments of ordered solids [1]. Surface applications of this theory have been restricted to approximate implementations [2] (non-self-consistent, using bulk-alloy scattering), and only recently fully implemented (in a related formalism) and used for disordered overlayers on metal substrates [3]. Charge self-consistency is essential in the description of many surface properties, e.g. energetics. In this regard the electronic work function Φ is important, being both very sensitive to the charge distribution and also experimentally measurable with good accuracy. For alloys, measurements of Φ during annealing are used to monitor surface aggregation [4]. In this letter I show that alloy work functions calculated within the CPA agree with experimental data, implying that this approximation describes well the layer-averaged charge distribution. Conclusion are drawn regarding screening at the alloy surfaces, and questions raised regarding the interpretation of Pd on Ag growth experiments.

The work function Φ is evaluated from [5]

$$\Phi = \Delta\phi - E_F \tag{1}$$

† Address for correspondence: TCM, Cavendish Laboratory, Madingley Road, Cambridge, CB3 0HE, UK. E-mail address: sc10016@phy.cam.ac.uk

0953-8984/93/360443+06$07.50

where E_F is the Fermi energy and $\Delta\phi$ is the difference in electrostatic potential across the surface region. For a semi-infinite sample of surface area NA ($N \to \infty$; A unit cell area) [6]

$$\Delta\phi = \frac{4\pi}{NA}\sum_{R}\left[\sqrt{4\pi}\,Q_R^{00}R_\perp + \sqrt{4\pi/3}\,Q_R^{10}\right] \tag{2}$$

where the multipoles associated with site $\boldsymbol{R} = (\boldsymbol{R}_\parallel, R_\perp)$ are

$$Q_R^{lm} = \int_{r\in S_R} \mathrm{d}^3\boldsymbol{r}\, Y_{lm}^*(\hat{\boldsymbol{r}}_R)r_R^l n(\boldsymbol{r}) - \frac{Z_R}{\sqrt{4\pi}}\delta_{l0}\delta_{m0} \tag{3}$$

with $\boldsymbol{r}_R = \boldsymbol{r} - \boldsymbol{R}$, $n(\boldsymbol{r})$ the electronic charge density and Z_R and S_R the nuclear charge and atomic cell at $\boldsymbol{R}$, respectively. For an ideal substitutional alloy where the atoms occupy a regular lattice the summation over $\boldsymbol{R}_\parallel$ is equivalent to performing a configurational average (denoted $\langle\ \rangle$) and

$$\Delta\phi = \frac{4\pi}{\mathrm{A}}\sum_{R_\perp}\left[\sqrt{4\pi}\langle Q_{R_\perp}^{00}\rangle R_\perp + \sqrt{4\pi/3}\langle Q_{R_\perp}^{10}\rangle\right]. \tag{4}$$

This forms the basis of the calculated Φ.

The multipoles are obtained from layer KKR [7] electronic structure calculations within the atomic sphere approximation (ASA) and using the CPA [8] for the random state. These also provide E_F from the charge neutrality condition. Details regarding the method may be found in [7, 9, 10]. Briefly, the Green function $G(\boldsymbol{r}, \boldsymbol{r}')$ is found by multiple scattering techniques using a layer-wise decomposition and subsequent resummation of scattering paths. The charge density $n(\boldsymbol{r}) = (1/\pi)\mathrm{Im}\ G(\boldsymbol{r}, \boldsymbol{r})$ is found self-consistently, so that the potential used to generate $n(\boldsymbol{r})$ is the same as the sum of the electrostatic potential $\phi(\boldsymbol{r})$ generated by $n(\boldsymbol{r})$ and the nuclear charges, and the exchange–correlation potential which is evaluated in the local-density approximation. In solving the Poisson equation, only charge and dipole contributions are included, and $G(\boldsymbol{r}, \boldsymbol{r}')$ is found using the spherical average of each atom-centred expansion of the potential. The utility of this approach was recently demonstrated by Skriver and Rosengaard [11] in elucidating the trends in elemental surface energies and work functions.

Random occupancy is accommodated via the CPA, with the site-diagonal Green function configurationally averaged through the condition that layer-concentration weighted scattering by impurities within the CPA medium vanishes:

$$\sum_{\alpha=\mathrm{Pd,Ag}} \mu_\alpha^i\left[\left(m_\alpha^i - m_C^i\right)^{-1} + \tau_C^i\right]^{-1} = 0. \tag{5}$$

Here, μ_α^i denotes the concentration and m the inverse-scattering matrix of species α, layer i, and m_C, τ_C are respectively the layer-dependent inverse-scattering matrix and scattering path operator of the CPA medium. Equation (5) applies to each layer within the solid, which are coupled via the renormalized propagator Δ in the expression for τ_C^n,

$$\tau_C^i = \frac{1}{\Omega}\int_\Omega \left[m_C^i - \mathcal{G}^i(\boldsymbol{k}_\parallel) - \Delta^i\left(\boldsymbol{k}_\parallel; \left\{m_C^j, j \neq i\right\}\right)\right]^{-1} \mathrm{d}\boldsymbol{k}_\parallel. \tag{6}$$

$\mathcal{G}$ is the intralayer structure constant. In practice, beyond three or four layers into the solid m_C^i may be fixed at the bulk value. Previous applications to alloys include the effects of interdiffusion on interface magnetism [9, 12] and alloy defect energies [13].

The calculations use spd partial waves and 13 plane waves for interlayer scattering. Valence band integrals use 16 points along a semi-circular contour and Brillouin zone integrals 45 special points within the 1/12th irreducible segment. All states are treated scalar relativistically. These parameters give good convergence (see also [14]), and the calculated lattice constants are $a_{Pd} = 3.91$ Å (experiment, 3.89 Å) and $a_{Ag} = 4.07$ Å (4.09 Å). For calculating Φ, experimental a were used and for the alloys Vegards law was assumed. No surface relaxations were considered (see table 1). Allowing the top three substrate layers and two vacuum layers to relax self-consistently gives $\Phi_{(111)}$ to < 5 meV. The values found for the pure metals are $\Phi_{Pd} = 5.59$ eV (experiment: 5.6 eV [15], 5.55 eV [16]) and $\Phi_{Ag} = 4.80$ eV (experiment: 4.69 eV, 4.74 eV [17]).

Table 1. Calculated work functions (in eV) for overlayer systems Pd/Ag(111) and Ag/Pd(111). For the ideal structure the overlayer adopts substrate interatomic spacings. The relaxed structure is given by touching bulk radii. For the latter the first value corresponds to all volume changes accommodated within the overlayer atomic sphere, and for the second it is shared equally between overlayer and interface atoms. Also shown are results for clean surfaces, relaxation indicating a 2% contraction in top-layer spacing (as an upper limit to assess the possible importance of structural relaxation) and results at different lattice constants.

	Ideal	Relaxed
Pd/Ag(111)	5.51	5.49, 5.51
Ag/Pd(111)	4.86	4.92, 4.91
Pd(111)	5.59	5.58, 5.59
Ag(111)	4.80	4.75, 4.75
Pd(111) at a_{Ag}	5.53	—
Ag(111) at a_{Pd}	4.99	—

Figure 1(a) shows $\Phi_{(111)}$ calculated for PdAg alloys. For crystals with uniform composition profile Φ deviates only slightly from linear dependance upon bulk Ag concentration, μ_{Ag}^B. Both $\Delta\phi$ and E_F (figure 1(b)) show more variation due to the competing effects of increasing volume and valency with rising Ag content. The variation of the dipole barrier (1.0 eV between the pure metal limits) dominates. In the Pd-rich regime the increasing volume is the major influence, inducing sp $\rightarrow$ d charge transfer and reducing E_F as the environment becomes more atomic like. (In the jellium model of metallic surfaces [5] $\Delta\phi \sim n$ to a good approximation. By their very nature it is the sp electrons which spill out, the tightly bound d electrons playing a more passive rôle.) Increasing valence becomes significant beyond $\mu_{Ag}^B \simeq 0.4$ when the 4d band is full. The trend in E_F is reversed as the density of levels accommodating subsequent charge increase is greatly reduced and the fall in $\Delta\phi$ partially resisted by the increasing sp charge count. However, since Φ depends upon $\Delta\phi - E_F$ these variations largely cancel.

For Ag-enriched surfaces, compositions are used consistent with Auger electron spectroscopy from supported polycrystalline catalysts [18]: these are bulk|surface Ag-concentrations $\mu_{Ag}^B|\mu_{Ag}^S = 0.25|0.55$, $0.50|0.725$ and $0.75|0.85$. The resulting $\Phi_{(111)}$ are lower than the ideal surface values so the concentration graph curves concavely below the linear interpolation between Φ_{Pd}, Φ_{Ag}. This is consistent with the value for polycrystalline Φ measured by Bouwman *et al* [19] (figure 1(c)) and the magnitude of curvature quantitatively correct. It is concluded that the configurationally averaged multipoles obtained within the

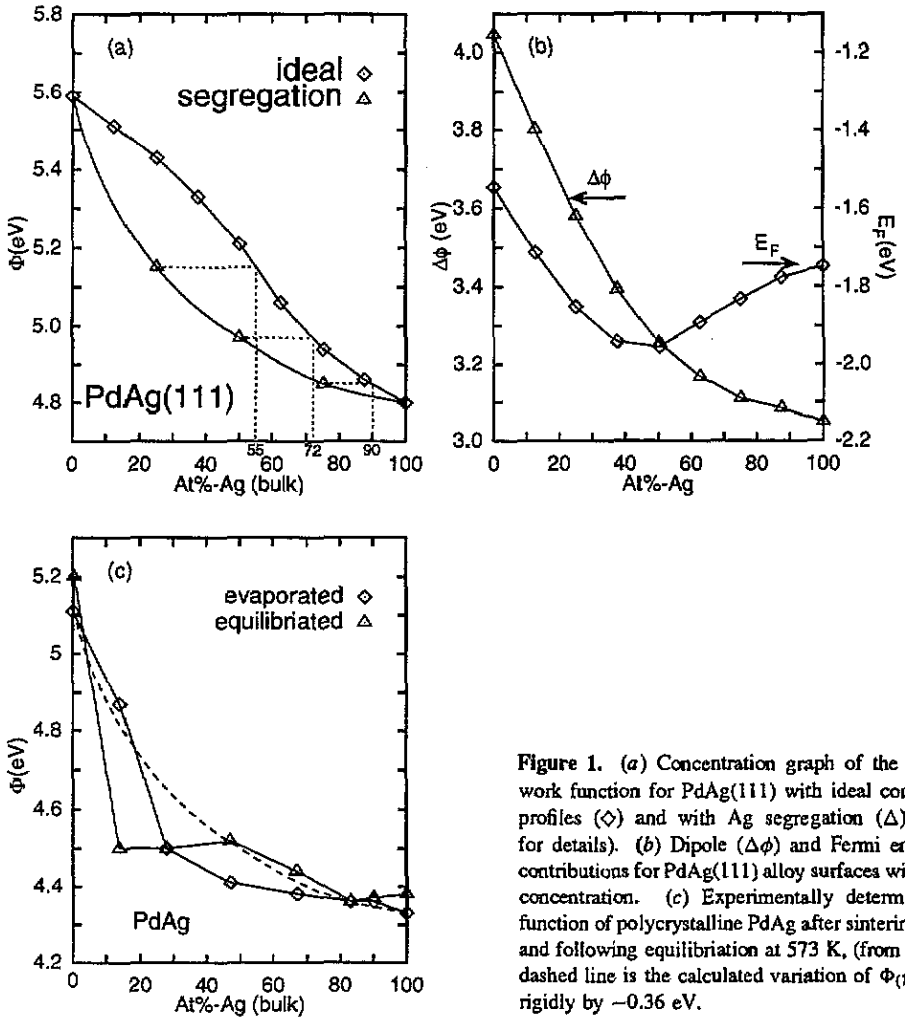

Figure 1. (*a*) Concentration graph of the calculated work function for PdAg(111) with ideal concentration profiles (◇) and with Ag segregation (△) (see text for details). (*b*) Dipole ($\Delta\phi$) and Fermi energy (E_F) contributions for PdAg(111) alloy surfaces with uniform concentration. (*c*) Experimentally determined work function of polycrystalline PdAg after sintering at 293 K and following equilibriation at 573 K, (from [21]). The dashed line is the calculated variation of $\Phi_{(111)}$ shifted rigidly by −0.36 eV.

CPA are accurate. This is despite both measured surface compositions and work functions refering to polycrystalline samples whereas this study concerns the (111) surface. Face-dependent work functions of Pd and Ag differ uniformly by ~0.8eV [20], whilst the arguments accounting for a linear variation of $\Phi_{(111)}$ with composition for ideal crystals apply to other surfaces. Hence, in the absence of segregation, the polycrystalline Φ would also vary linearly with composition. Also, it is evident in figure 1(*a*) that for enriched surfaces Φ is similar in value to that of crystals with uniform composition and the same Ag content as at the surfaces of the former, so, for non-uniform concentration profiles, Φ is a good measure of surface composition. This is confirmed by calculations for other concentration profiles, including multilayer segregation which show Φ is essentially independent of subsurface concentration. Examples are the systems with (S−1 denotes subsurface layer) $\mu^{B}_{Ag}|\mu^{S-1}_{Ag}|\mu^{S}_{Ag} = 0.50|0.725|0.725$, for which $\Phi = 4.97$ eV is found, and $\mu^{B}_{Ag}|\mu^{S-1}_{Ag}|\mu^{S}_{Ag} = 0.25|0.10|0.55$, for which $\Phi = 5.20$ eV. Thus the agreement in the magnitude of curvature is consistent with the use of the polycrystalline surface compositions.

These results are in accord with disordered overlayer calculations PdAg/Ag(001) where

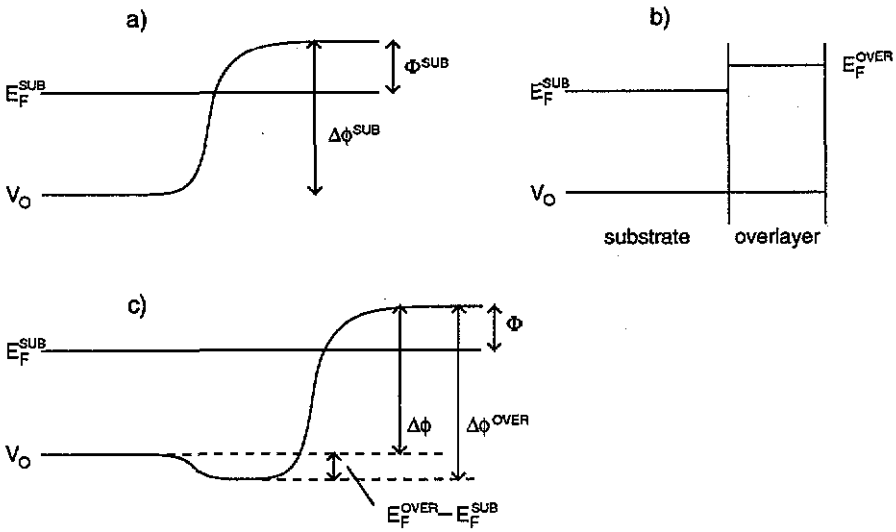

Figure 2. (*a*) Energy diagram of the clean surface. A similar diagram applies to the overlayer material. (*b*) Potential line-up in the atomic sphere approximation, before self-consistency. (*c*) Energy diagram for the overlayer system, accounting for Φ being independent of the substrate Fermi level.

$\Phi - \Phi_{Pd}$ was found proportional to the surface Ag concentration [3]. Apparantly, Φ is independant of the number of surface layers ($\geqslant 1$) of concentration μ_{Ag}^{S} and of the substrate composition, and hence independant of the bulk contribution to the work function E_F, equation (1). This paradox is due to efficient screening, as illustrated by the energy diagrams in figure 2. Imagine the surface potential for an overlayer (or enriched selvedge region) constructed in two stages, cutting around the cell potentials of the respective bulk materials and rigidly pasting together, figure 2(*b*), and then allowing self-consistent relaxation. Within the ASA the bulk potentials are referenced to a common energy zero, V_0, whilst the respective Fermi levels of substrate and overlayer are different, driving charge transfer during self-consistency creating a dipole barrier of height $E_F^{OVER} - E_F^{SUB}$ at the interface to equilibriate them. If the screening length is shorter than the overlayer thickness and no mutual interaction occurs between interfacial and surface dipole barriers, the energy diagram in figure 2(*c*) applies and

$$\Phi = \Delta\phi - E_F^{SUB} = \Delta\phi^{OVER} - (E_F^{OVER} - E_F^{SUB}) - E_F^{SUB} = \Phi^{OVER}. \qquad (7)$$

Under these conditions Φ is that of the overlayer material. For the PdAg system this holds well on the monolayer (ML) scale, implying a very short screening length. Note the relevant Fermi energy for the overlayer is that evaluated at the substrate lattice dimension, which for the present case gives Ag→Pd charge transfer. The lattice constants of Ag and Pd differ by $\sim 5\%$ but Φ_{Ag} is not sufficiently sensitive to this—and Φ_{Pd} not at all—to significantly modify the situation, see table 1.

Calculated and measured work functions for several other ordered metal-on-metal systems, e.g. Au/Cr(001) [21], Co/Au(001) [22], Ag/Fe(001) [23] and Cu/Ru(0001) [24] also indicate Φ close to that of the overlayer species for coverages $\Theta \geqslant 1$ ML. In contrast, Φ measured during the growth of Pd/Ag increases gradually, reaching saturation only for

$\Theta \simeq 8$ ML [25]. The results for the alloy and overlayer (table 1) systems reported here indicate this is inconsistent with the layer-by-layer growth of a Pd film [25], which would lead to a rapid rise of Φ with Θ, but point to the likely formation of a less Pd-rich surface alloy phase. Interestingly, it has been inferred recently that the growth of Pd on Al(111), for which $\Phi(\Theta)$ shows a similar evolution [26], initially proceeds through just such an alloy formation [27].

To summarize, it has been shown that work functions of PdAg random alloys calculated within the CPA are in good agreement with experiment, indicating an accurate description of the layer-averaged charge distribution and hence the possibility of an *ab initio* description of other surface-related alloy properties. These results also indicate that work function changes measured during the thermal treatment of alloys, currently used to determine the nature of the segregating species [4], may, in conjunction with similar calculations to these, be used for a quantitative measure of surface enrichment. It has also been suggested that the growth of Pd on Ag involves the formation of an alloy phase at the surface.

This work was supported by the Stichting voor Fundamenteel Onderzoek der Materie.

References

[1] Johnson D D, Nicholson D M, Pinski F J, Gyorffy B L and Stocks G M 1985 *Phys. Rev. Lett.* **56** 2088
[2] See, e.g.
Wille L T and Durham P J 1985 *Surf. Sci.* **164** 19
[3] Kudmovský J, Turek I, Drchal V, Weinberger P, Christensen N E and Bose S K 1992 *Phys. Rev.* B **46** 4223
[4] See, e.g.
Weigand P, Novacek P, van Husen G, Neidhart T and Varga P 1992 *Surf. Sci.* **269/270** 1129
[5] Lang N D and Kohn W 1971 *Phys. Rev.* B **3** 1215
[6] Skriver H L and Rosengaard N M 1991 *Phys. Rev.* B **43** 9538
[7] MacLaren J M, Crampin S, Vvedensky D D and Pendry J B 1989 *Phys. Rev.* B **40** 12 164
[8] Faulkner J S and Stocks G M 1980 *Phys. Rev.* B **21** 3222
[9] Crampin S, Monnier R, Schulthess T, Schadler G H and Vvedensky D D 1992 *Phys. Rev.* B **45** 464
[10] Crampin S 1993 *J. Phys.: Condens. Matter* **5** 4647
[11] Skriver H L and Rosengaard N M 1992 *Phys. Rev.* B **46** 7157
[12] Schulthess T, Crampin S and Monnier R 1993 *Solid State Commun.* at press
[13] Crampin S, Monnier R and Vvedensky D D 1993 *Phil. Mag.* A **67** 1447
[14] Crampin S, Hampel K, Vvedensky D D and MacLaren J M 1990 *J. Mater. Res.* **5** 2107
[15] Demuth J E 1977 *Surf. Sci.* **65** 369
[16] Eastman D E 1970 *Phys. Rev.* B **2** 1
[17] Straub D and Himpsel F J 1986 *Phys. Rev.* B **33** 2256, and references therein
[18] Wood B J and Wise H 1975 *Surf. Sci.* **52** 151
[19] Bouwman R, Lippits G J M and Sachtler W M H 1972 *J. Catal.* **25** 350
[20] Methfessel M, Hennig D and Scheffler M 1992 *Phys. Rev.* B **46** 4816
[21] Feibelman P J and Hamann D R 1984 *Phys. Rev.* B **29** 6463
[22] Heinen W, Carbone C, Kachel T and Gudat W 1990 *J. Electron Spectrosc. Relat. Phenom.* **51** 701
[23] Ohnishi S, Weinert M and Freeman A J 1984 *Phys. Rev.* B **30** 36
[24] Housten J E, Peden C H F, Blair D S and Goodman D W 1986 *Surf. Sci.* **167** 427
[25] Smith G C, Norris C, Binns C and Padmore H A 1982 *J. Phys. C: Solid State Phys.* **15** 6481
[26] Frick B and Jacobi K 1988 *Phys. Rev.* B **37** 4408
[27] Smith R J, Denier van der Gon A W and van der Veen J F 1988 *Phys. Rev.* B **38** 12 712